Open Archive Toulouse Archive Ouverte (OATAO)

OATAO is an open access repository that collects the work of Toulouse researchers and makes it freely available over the web where possible

This is an author's version published in: **http://oatao.univ-toulouse.fr/23619**

Any correspondence concerning this service should be sent to the repository administrator: tech-oatao@listes-diff.inp-toulouse.fr

Materials Research Express

PAPER

Effect of van der Waals corrections on DFT-computed metallic surface properties

Fatah Chiter[1,2], **Van Bac Nguyen**[2], **Nathalie Tarrat**[2], **Magali Benoit**[2], **Hao Tang**[2] and **Corinne Lacaze-Dufaure**[1]

1   CIRIMAT, Université de Toulouse, CNRS, INPT, UPS, ENSIACET 4, allée Emile Monso BP F-44362, 31030 Toulouse cedex 4, France
2   CEMES, Université de Toulouse, CNRS, UPS, 29 Rue Jeanne Marvig, F-31055 Toulouse Cedex 4, France

E-mail: corinne.dufaure@ensiacet.fr

Abstract

State-of-the-art van der Waals (vdW) corrected density functional theory (DFT) is routinely used to overcome the failure of standard DFT in the description of molecule/surface long range interactions. However, the systematic use of dispersion forces to model metallic surfaces could lead to less accurate results than the standard DFT and the effect of these corrections on the metal properties should be properly evaluated. In this framework, the behavior of two widely used vdW corrected DFT methods (DFT-D2 and vdW–DF/optB86b) has been evaluated on six metals, i.e. Al, Cu, Au, Ni, Co and Fe, with respect to standard GGA–DFT and experiments. Regarding bulk properties, general trends are found for the lattice parameter, cohesive energy and magnetic moment variations when the vdW correction is introduced. Surface energies, work functions and interlayer distances of closed packed surfaces, Al(111), Cu(111), Au(111) and magnetic Ni(111), Co(0001) and Fe(110), are also strongly affected by the dispersion forces. These modifications suggest a systematic verification of the surface properties when a dispersion correction is included.

1. Introduction

London dispersion forces, usually referred as 'van der Waals (vdW) forces', originate from the instantaneous interaction between dipoles induced by charge fluctuation. These interactions, varying as $-1/r^6$ decay [1], are missing in standard exchange-correlation (XC) functionals used in density functional theory (DFT). This deficiency was one of the main obstacles encountered by DFT methods to properly describe weakly bonded materials or the adsorption of molecules on surfaces. Moreover it was also demonstrated that the dipole–dipole vdW forces contribute to the total cohesive energy in metals [2–5].

While solutions have been proposed to take into account dispersion forces in DFT calculations since the mid of 90s, significant efforts in that regard were undertaken only within the past decade. In this framework, weakly bonded systems were mostly investigated and were used as benchmark datasets (S22 [6, 7], S66 [7], X23 [8]) for the validation of the proposed vdW correction methods. As a result, the description of rare gases or molecular crystals was significantly improved [9]. Considering the benefit of such vdW corrected DFT methods, they were widely used for modeling the adsorption of molecules on metallic surfaces and several reviews were proposed in the literature [7, 9–14]. For instance, Tkatchenko *et al* [15, 16] pointed out that a modeling of the structure and stability of hybrid systems using dispersion corrected functionals is reliable and required. Indeed, an accurate description of the molecule-surface interaction is mandatory for explaining and forecasting the behavior of molecules on metals, in various fields such as catalysis, stabilization of nanoparticles, surface functionalization, or even in surface protections or nanotechnology. However, in spite of a quasi-systematic use of vdW corrections in recent DFT studies of molecule-surface systems, the effect of the introduction of such a correction on the metallic surfaces has been under-researched. We found important to point out the modifications of the surface properties induced by such corrections.

For bulk materials, Klimeš *et al* [17, 18] and Carrasco *et al* [19], have shown a good behavior of optB86b, their modified vdW density functional (vdW–DF) on lattice parameter, bulk modulus and atomization energy of

different materials such as some noble metals, transition metals, alkali and alkaline-earth metals, ionic crystals, oxide and semiconductors. In 2013, Schimka *et al* [20] have computed the lattice constants and cohesive energies of a series of alkali, alkaline-earth and transition metals with the random phase approximation (RPA) and with a vdW corrected DFT method (optB88-vdW). The sophisticated RPA method gave the lowest errors when compared with experiments but this approach is too computationally demanding to be applied on large surface models such as those used for studying molecular adsorption. The optB88-vdW functional scored less well as it seemed to overestimate the dispersion forces in alkali and alkaline earth metals and thus lead to underestimated lattice parameters for these solids. However, Ding *et al* [21] showed that the same functional gave results particularly close to experimental counterpart for the bulk properties and plasticity of magnesium. Bucko *et al* [22] have compared the vdW correction method proposed by Tkachenko and Scheffler [23] with and without self-consistent screening (TS-SC) on different solids including rare gas solids (Ne, Ar, Kr, Xe), molecular solids (α N_2, sulfur dioxide, benzene, naphthalene and cytosine), layered materials and chain-like structures (graphite, hexagonal boron nitride, vanadium pentoxide, MoS_2 and $NbSe_2$), materials with chain-like structures (selenium, tellurium, cellulose I-β), ionic crystals and metals (nickel, zinc, cadmium). They found that the calculated structures are in good agreement with experiment but that the vdW corrections often overestimated the binding energies. They pointed out that the TS-SCS approach leads to significantly better results in some problematic cases.

For surfaces, very few studies have assessed the quality of the data (lattice parameter and/or bulk modulus and/or surface relaxation) obtained using vdW-corrected DFT methods [10, 24, 25]. Moreover, in these studies, these parameters were evaluated only for the method they used for studying the adsorption. To our knowledge, only one study describes a comparison of the surface energy and relaxation of different facets of a given metal obtained with and without a dispersion correction [26, 27]. The purpose of this work is neither to give an exhaustive list of the metal surface properties obtained using all the existing corrections, nor to seek for the best vdW corrected functional for describing a given metal surface. It is rather intended to show the typical modifications one could expect on the surface properties arising from the use of vdW corrected functionals.

To this end, we have evaluated the effect of dispersion corrections on the surface properties of six compact metallic surfaces, i.e. Al(111), Cu(111), Au(111), Ni(111), Co(0001) and Fe(110). Five of the six metals studied are transition metals and all have been chosen because of their frequent use as molecular adsorption substrates or as stable facets of nanoparticles [28–30]. We tested one example for each of the two most representative classes of vdW correction methods (non-local correlation functional and semi-empirical additive DFT-D). After the verification on lattice parameter, bulk modulus and cohesive energy for the bulk, we have focused on surface energy, surface relaxation and work function of these surfaces. For magnetic metals, the magnetic properties have also been computed. These results provide an indication of the modification of the surface properties arising from taking into account the dispersion forces.

2. Computational details and models of the surfaces

Calculations in the framework of the DFT were performed by using the Vienna *ab initio* simulations package (VASP) [31–33], a plane-wave basis implementation of DFT. Pseudopotentials based on the projector augmented wave (PAW) method [34, 35] which allows an accurate description of the electronic structure were used with different functionals. As a reference, lattice parameter, cohesive energy, bulk modulus, surface energy, surface relaxation and work function were calculated at first with the well known Perdew–Burke–Ernzehof (PBE) [36] functional in the generalized gradient approximation (GGA). These quantities were then compared to that evaluated with vdW corrected DFT. Among the semi-empirical corrections, we selected the DFT-D2 method proposed by Grimme [37], which consists in adding a pair wise potential to the DFT total energy after each self-consistent cycle.

$$E = E_{KS} + E_{\text{disp}} \tag{1}$$

and

$$E_{\text{disp}} = -S_6 \sum_{i}^{N-1} \sum_{j=i+1}^{N} \frac{C_6^{ij}}{(R^{ij})^6} F_{\text{dmp}}(R^{ij}) \quad \text{dispersion term,} \tag{2}$$

$$F_{\text{dmp}}(R^{ij}) = \frac{1}{1 + e^{-d\left(\frac{R^{ij}}{R_0^i + R_0^j - 1}\right)}} \quad \text{damping function,} \tag{3}$$

$$C_6^{ij} = \sqrt{C_6^i C_6^j} \quad \text{dispersion coefficient,} \tag{4}$$

where S_6 is a global scaling factor, R^{ij} the distance between atoms i and j, d a damping parameter, C_6^i the atomic parameter and R_0^i the vdW radius of atom i. Note that the C_6^i and R_0^i parameters are identical for Fe, Co and Ni.

Table 1. Parameters used for the bulk calculations. E_{cut} is the cutoff energy, k-points is the size of the k-points grid $(n \times n \times n)$.

Metal	E_{cut} (eV)	k-points
Al	450	$15 \times 15 \times 15$
Cu	500	$17 \times 17 \times 17$
Au	600	$19 \times 19 \times 19$
Co	650	$21 \times 21 \times 21$
Ni	600	$19 \times 19 \times 19$
Fe	400	$18 \times 18 \times 18$

In the Grimme correction method, the parameters C_6^i and R_0^i were obtained by fitting experimental data [37]. For this class of correction methods, Tkatchenko and Scheffler proposed to obtain these same parameters from the electron density [23].

Among the non-local functionals, also called vdW–DF [38], we selected the optB86b one, a functional optimized by Klimeš et al [18], and known for its ability to describe structural properties of solids. In this method, the vdW interaction is considered implicitly by the nonlocal contribution of the electronic density

$$E_{xc}^{vdW-DF}[\rho(\vec{r})] = E_x^{GGA}[\rho(\vec{r})] + E_c^{LDA}[\rho(\vec{r})] + E_c^{nl}[\rho(\vec{r})]. \tag{5}$$

2.1. Bulk calculations

For bulk materials, the convergence (less than 1 meV per atom) with respect to the cutoff energy (E_{cut}), Methfessel–Paxton smearing σ [39] and size of the Monkhorst–Pack mesh of k-points [40] was carefully checked for each system. The calculation parameters used are presented in table 1. The value of the smearing σ was taken to 0.05 eV for all metals.

By fitting the total energy versus the lattice volume using equation (6), the optimized lattice parameters were deduced from the volume at the minimum energy:

$$E_{bulk} = a_0 + a_1 V + a_2 V^2, \tag{6}$$

where E_{bulk} is the energy of the unit cell with N atoms and V the volume of the unit cell.

Cohesive energies E_{coh} per atom were calculated using equation (7):

$$E_{coh} = \frac{E_{bulk}}{N} - E_{atom}, \tag{7}$$

where E_{atom} is the energy of the isolated atom in vacuum.

The bulk modulus B_0 measures the volume variation due to external pressure. It is defined as in equation (8). This quantity was calculated by using the Murnaghan equation of state [41]

$$B_0 = -V_0 \left(\frac{\partial P}{\partial V} \right)_T \tag{8}$$

2.2. Surfaces calculations

For surface calculations, symmetric slabs were chosen. The height of the vacuum region was checked to minimize the interaction between periodic slabs in the z-direction. The total surface energies were calculated with the same accuracy as the bulk, but using $(n \times n \times 1)$ k-points grid, n being given in table 1. That leads to good convergence of the surface energy [42]. The number of atomic layers was gradually increased to get the convergence of the surface energy ($\Delta\gamma < 0.005$ eV atom^{-1}) and convergence of the interplanar distance variation in the middle of the slab (see figure 6). The number of atomic layers was 19 layers for the Al, Cu and Au slabs, 15 layers for Co and Ni metals and 20 layers for the Fe slab.

All atoms were fully relaxed with the conjugate gradient algorithm until forces on each of them were less than 0.001 eV Å^{-1}. Spin polarization was taken into account for magnetic materials, i.e. Ni, Co and Fe.

The surface energy γ for a symmetric slab was calculated using:

$$\gamma = \frac{E_{slab} - n\dfrac{E_{bulk}}{N}}{2A}, \tag{9}$$

Table 2. Calculated and experimental lattice parameters a_0 (Å) for fcc and bcc, a_0/c_0 for hcp crystals.

Metal	PBE	DFT-D2	optB86b	Exp. [43]
Al(fcc)	4.037	4.008	4.031	4.04/4.05
Cu(fcc)	3.635	3.570	3.597	3.61
Au(fcc)	4.174	4.096	4.138	4.08
Ni(fcc)	3.525	3.464	3.494	3.52
Co(hcp)	2.491/	2.463/	2.472/1.616	2.51/1.62
	1.625	1.600		
Fe(bcc)	2.835	2.804	2.807	2.87

where E_{slab} is the total energy of the fully relaxed slab, n the number of metallic atoms in the supercell and A is the surface area of the slab.

The relaxation of the surfaces was described by the interlayer distances variation:

$$\Delta d_{ij} = \frac{d_{ij} - d_{\text{bulk}}}{d_{\text{bulk}}} \times 100\%, \tag{10}$$

where d_{ij} are the interlayer distances and i and j the index of the atomic layers from the surface, i.e. d_{12} is the distance between the surface (index 1) and the subsurface (index 2) layers. d_{bulk} is the interlayer distance in the bulk.

The work function ϕ is the minimum energy required to extract an electron from the surface to the vacuum. Work function changes $\Delta \phi$ are particularly studied for the adsorption processes on metal surfaces. We calculated the work function of the metals from the difference between the Fermi energy of the system and the electrostatic potential energy in the middle of the vacuum region. ϕ is thus given by:

$$\phi = V_{\infty} - E_{\text{F}}, \tag{11}$$

where E_{F} is the Fermi energy of the system and V_{∞} is the electrostatic potential in the vacuum. No dipole correction was necessary as we used symmetric slab models.

3. Results and discussions

3.1. Bulk

The equilibrium lattice parameters obtained by using the PBE, DFT-D2 and optB86b functionals are summarized in table 2. The general trend of the a_0 variation is a graduated shift to smaller values from PBE to optB86b and finally to DFT-D2 as shown in figure 1. This behavior of the lattice parameters agrees with literature results [18, 19]. The authors showed that the optB86b-vdW functional gives smaller lattice parameters than the PBE functional for all metals. The results obtained by optB88-vdW are not constant: the calculated lattice parameters are similar using optB88 and PBE functionals for transition metals, whereas the optB88 functional gives worst lattice parametres than the PBE functional for alkali and alkali-earth metals. In the present study, for fcc Al and Ni, hcp Co and bcc Fe, the lattice parameters calculated with PBE best agree with the experimental values. For Cu, the best agreement was obtained with optB86b with $\Delta a_0 = -0.4\%$, whereas for Au the a_0 calculated with DFT-D2 gives a deviation Δa_0 of $+0.4\%$. Therefore the inclusion of vdW forces in the calculation tends to decrease the volume of the unit cell at 0 K for all studied metals.

The variation of the bulk modulus B_0 is presented in table 3 and in figure 2. The analysis of the results of our computations shows a shift of B_0 to larger values with the optB86b functional and DFT-D2 corrections for Cu, Au, Ni and Co, following thus the expected trend. On the contrary, the value of B_0 is decreased for Al when we turn from PBE to dispersion corrected methods and for Fe when the optB86b functional is used. For three of the six studied metals (Cu, Ni, Co), the PBE functional gives the results that are in best agreement with their experimental counterparts. For Al, Au and Fe, the best approach for the calculation of the bulk modulus is the DFT-D2 one. The lack of clear trend for the variation of the bulk modulus with the functional might be attributed to the well-known DFT error (with or without dispersion correction) which is around $\pm 20\%$, for standard calculations. One could improve the agreement of the calculated bulk modulus with experiment by increasing the accuracy of the calculation (finer k-points grid and higher cutoff). However, since the main purpose of this paper is to show the effects of the vdW corrected DFT methods on the metal properties compared to standard PBE, we decided to work at the same standard level of accuracy for all functionals.

The calculated value of the cohesive energy of a given metal is also method dependent. The cohesive energy calculated without and with vdW corrections are presented in table 4 and compared to the experimental values.
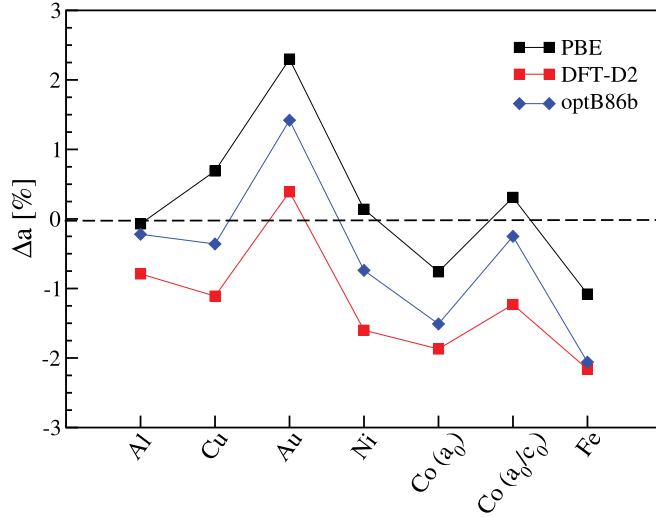
Figure 1. Deviation of the calculated lattice parameters from the experimental values, $\Delta a_0 = (a_0 - a_0^{\text{exp}}) \times 100/a_0^{\text{exp}}$ (and a_0/c_0 for Co).

Table 3. Calculated and experimental bulk moduli B_0 (GPa).

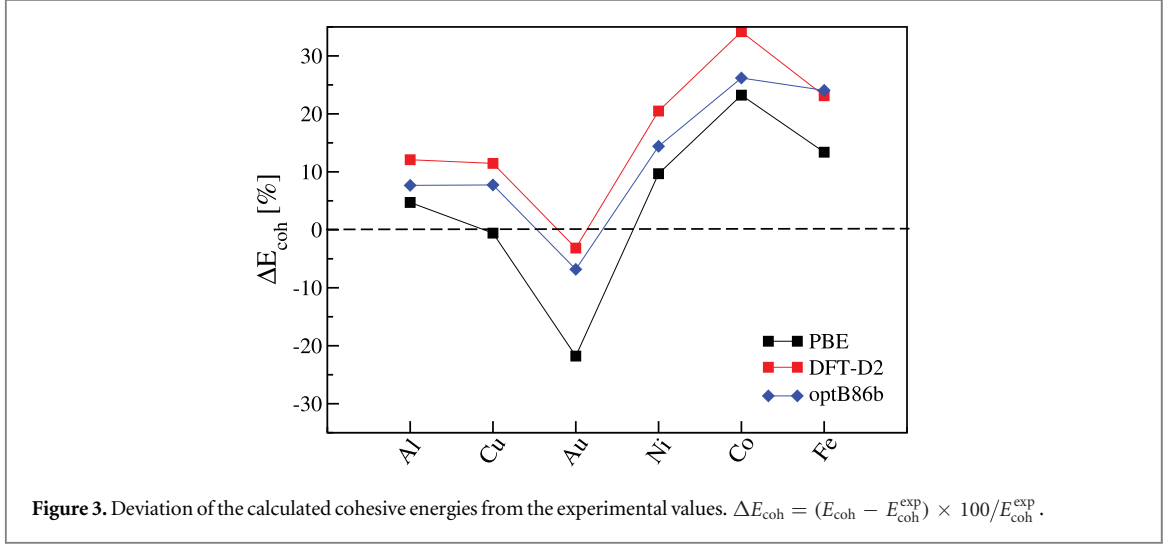| Metal	PBE	DFT-D2	optB86b	Exp. [43]
Al(fcc)	80	71	79	72
Cu(fcc)	139	144	149	137
Au(fcc)	136	154	146	173
Ni(fcc)	195	219	209	186
Co(hcp)	201	211	208	191
Fe(bcc)	186	176	199	168
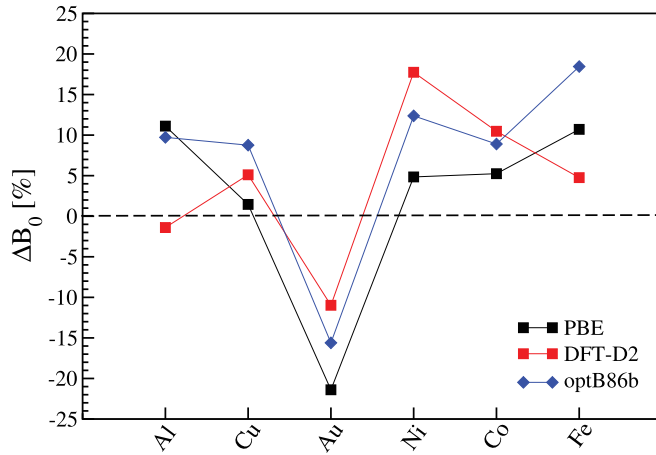
Figure 2. Deviation of the calculated bulk moduli from the experimental values. $\Delta B_0 = (B_0 - B_0^{\text{exp}}) \times 100/B_0^{\text{exp}}$.

DFT is known to estimate reasonably well this quantity [18, 20]. In agreement with the previous studies [2, 3], taking into account dispersion interactions increases the cohesion of the metallic bulks. In figure 3, the general trend is that $|E_{\text{coh}}^{\text{PBE}}| < |E_{\text{coh}}^{\text{optB86b}}| < |E_{\text{coh}}^{\text{DFT}-D2}|$, except for Fe for which the calculated optB86b and PBE-D2 cohesive energies are similar. This variation of the cohesive energy is similar to the variation already shown for the lattice parameter because, for a given metal, the values of the lattice parameter and of the cohesive energy are in close relation: smaller a_0 lead to higher E_{coh} (in absolute value). The minimum deviation to experimental values is for Cu with a relative error of −0.57% (PBE), while the largest deviation is for Co, with a relative variation of +34.17% (DFT-D2).

Table 4. Calculated and experimental cohesive energies (eV).

Metal	PBE	DFT-D2	optB86b	Exp. [43]
Al(fcc)	−3.55	−3.80	−3.65	−3.39
Cu(fcc)	−3.47	−3.89	−3.76	−3.49
Au(fcc)	−2.98	−3.69	−3.55	−3.81
Ni(fcc)	−4.87	−5.35	−5.08	−4.44
Co(hcp)	−5.41	−5.89	−5.54	−4.39
Fe(bcc)	−4.85	−5.27	−5.31	−4.28

Figure 3. Deviation of the calculated cohesive energies from the experimental values. $\Delta E_{coh} = (E_{coh} - E_{coh}^{exp}) \times 100/E_{coh}^{exp}$.

Table 5. Calculated and experimental atomic magnetic moment in μ_B/at.

Metal	PBE	DFT-D2	optB86b	Exp.
Ni(fcc)	0.65	0.59	0.58	0.61 [44]
Co(hcp)	1.61	1.55	1.56	1.71(at 77 K) [45]
Fe(bcc)	2.21	2.15	2.12	2.22 [44]

In the literature, Klimeš *et al* [18] computed these same quantities for Al and Cu using the PBE and optB86b. Their values for the lattice parameters, bulk modulus and cohesive energies were slightly different than ours due to slight differences in the computational conditions (number of k-points and E_{cut}). These properties have been calculated for many solids using several vdW density functional methods. The cohesive properties for alkali metals and alkali halides were improved by including dispersion non-local correlation term [18, 20].

For magnetic materials (Ni, Co and Fe), the atomic magnetic moments calculated with PBE, optB86b and DFT-D2 are compiled in table 5. The PBE functional gives values of the atomic magnetic moment that are decreased when using dispersion corrected methods. This is simply due to the fact that these methods decrease the lattice parameter for a given metal (compared to the PBE functional), and therefore the hybridization between the orbitals of neighbouring atoms is increased inducing a decrease of the magnetic moments.
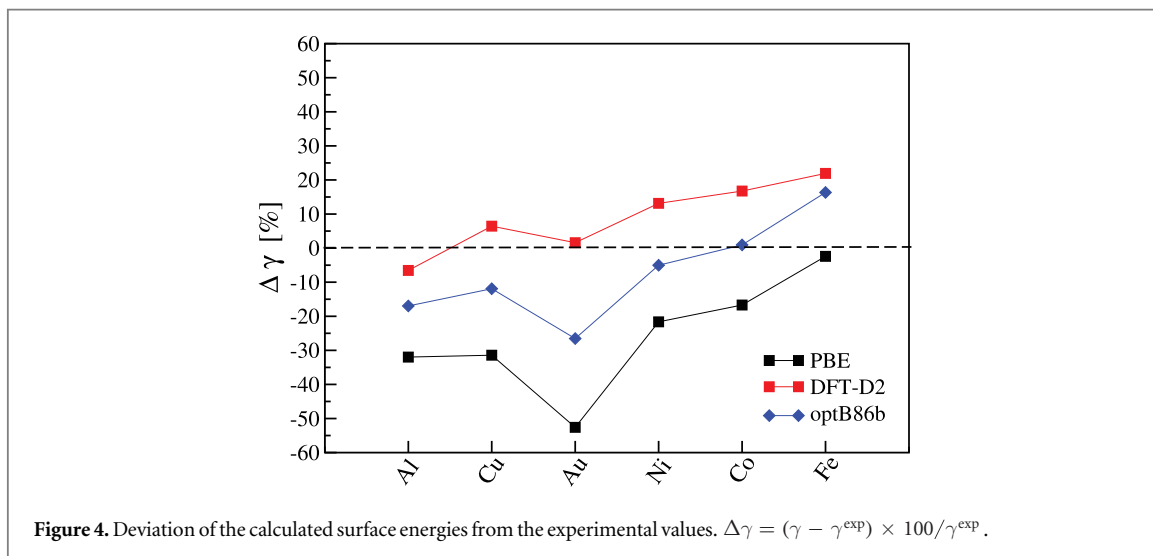
To sum up, in comparison to PBE results, the application of vdW corrections in the semi-empirical scheme (DFT-D2) or with the non-local functional approach (optB86b) decreases the lattice parameter and increases the cohesive energy (in absolute value), inducing a decrease of the atomic magnetic moments for the magnetic materials. The bulk modulus is also modified by the use of these functionals but no general trend was found.

Globally, we can conclude that the use of dispersion corrected methods modifies the calculated properties of the six studied metals. Depending on the performance of the PBE functional for a given metal, the use of a vdW functional might improve the agreement with experiment or deteriorate it. Note that, for Au, the PBE functional, as well as all gradient corrected exchange and correlation functionals, does not take into account the spin–orbit coupling and then leads to inaccurate results for the lattice parameters and the bulk modulus. In that case, the correction induced by taking into account the dispersion forces compensates artificially the error coming from the lack of spin–orbit coupling.

Table 6. Calculated surface energies γ in J m^{-2} and deviation from the experimental values.

Metal	PBE		DFT-D2		optB86b		Exp. [46]
	γ [J m^{-2}]	Error [%]	γ [J m^{-2}]	Error [%]	γ [J m^{-2}]	Error [%]	
Al(111)	0.78	−31.98	1.08	−6.55	0.96	−16.98	1.16
Cu(111)	1.25	−31.42	1.95	+6.44	1.61	−11.91	1.83
Au(111)	0.71	−52.60	1.52	+1.60	1.10	−26.53	1.50
Ni(111)	1.92	−21.63	2.77	+13.14	2.33	−5.02	2.45
Co(0001)	2.12	−16.70	2.98	+16.74	2.57	+0.94	2.55
Fe(110)	2.42	−2.42	3.02	+21.93	2.89	+16.33	2.48

Figure 4. Deviation of the calculated surface energies from the experimental values. $\Delta\gamma = (\gamma - \gamma^{\text{exp}}) \times 100/\gamma^{\text{exp}}$.

3.2. Surface properties

When a surface is created by cutting a solid, the atoms in and close to the surface tend to relax in order to minimize the surface energy and surface strains. By the same time, the surface electronic structure as well as the surface reactivity are modified consequently. It is thus of prime importance for DFT simulations to reproduce correctly surface properties. In this study, only the most close-packed orientations were considered for each metal, i.e. Al(111), Cu(111), Au(111), Ni(111), Co(0001) and Fe (110). To describe these surfaces, we used symmetric slabs as described in the 'computational details' section.

The calculated surface energies are summarized in table 6. For all the metals, the dispersion corrected methods give a surface energy that is higher than the PBE values. The DFT-D2 approach gives accurate results for the Al(111), Cu(111) and Au(111) surfaces, whereas the optB86b functional describes well the surface energy of the Ni(111) and Co(0001) surfaces. The PBE functional gives results in best agreement with experimental value only for the Fe(110) surface. Looking at figure 4, one can see that the dependence of the surface energies on the functionals is similar to that of the cohesive energies in bulk materials ($\gamma_{\text{PBE}} < \gamma_{\text{optB86b}} < \gamma_{\text{DFT-D2}}$). From the definition of the surface energy (equation (9)), one can try to understand these method dependent variations. Taking into account dispersion forces decreases the lattice parameter a_0, therefore the surface area, and increases the cohesive energy (in absolute value). Thus the increase in surface energy observed in dispersion corrected DFT compared to PBE can be explained by changes in the bulk properties.

As different vdW corrections significantly modify the bulk properties and the surface energies, we expect to find noticeable differences for the work function from one method to the other. For the six metallic surfaces investigated in the present work, the work functions are presented in table 7. The general variation trend here is $\Phi_{\text{PBE}} \leqslant \Phi_{\text{DFT-D2}} < \Phi_{\text{optB86b}}$ (see figure 5). The PBE and DFT-D2 methods give similar results and the best agreement with experiment for the Co(0001) and Fe(110) surfaces whereas the optB86b functional describes better the (111) surface of the Al, Cu, Au and Ni metals. Tkatchenko *et al* also noticed an increase of the work function for the (111) surface of Cu, Rh and Au when applying the self-consistent PBE+vdW correction [47]. This variation is indeed linked to the change in the surface electronic density description. As the electronic redistribution is at the origin of the surface relaxation [48], we also studied in details the dependence of the surface relaxation of the slab on the method.

Table 7. Calculated and experimental work function Φ in eV.

Metal	PBE	DFT-D2	optB86b	Exp. [46]
Al(111)	4.05	4.05	4.18	4.24
Cu(111)	4.76	4.82	4.98	4.94
Au(111)	5.09	5.17	5.32	5.31
Ni(111)	5.09	5.11	5.27	5.35
Co(0001)	4.91	4.91	5.17	5.00
Fe(110)	4.75	4.78	5.00	4.50
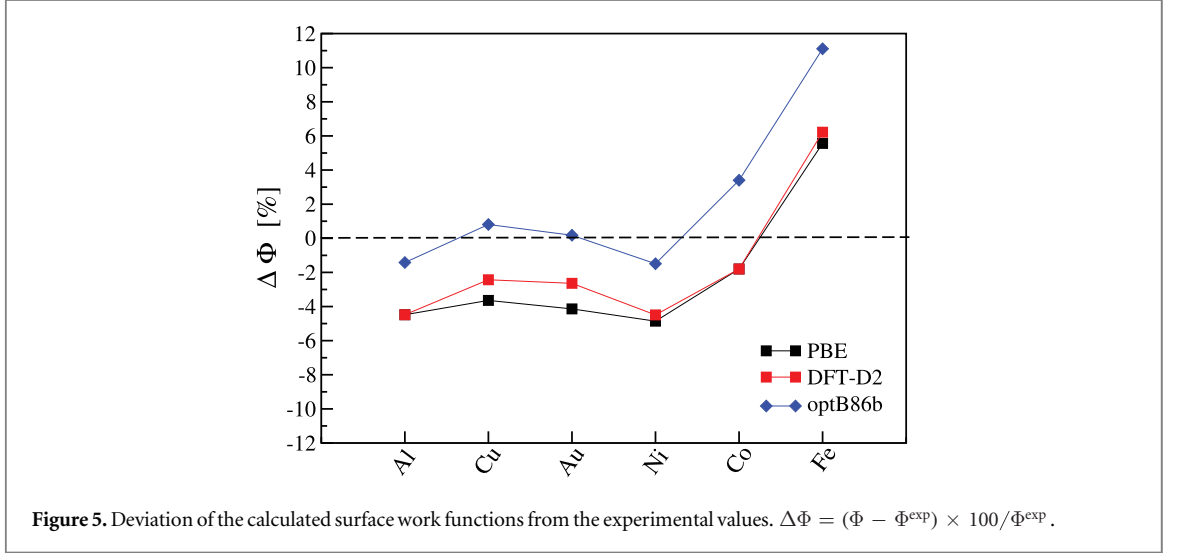
Figure 5. Deviation of the calculated surface work functions from the experimental values. $\Delta\Phi = (\Phi - \Phi^{exp}) \times 100/\Phi^{exp}$.

In the middle of the slabs, the interlayer distance should converge to its value in the bulk. In figure 6, the deviation of the interlayer distances Δd_{ij} as defined in equation (10) are presented for the six studied surfaces and for the three functionals. One can notice that the interlayer distances converge to their bulk values for Ni(111) whatever the calculation method used and for Fe(110) in the case of optB86b and PBE calculations. The largest deviation is obtained for Al(111) with an interlayer distance variation of $+1.0\%$ relatively to the bulk with the three functionals. To reach the bulk value, the number of atomic layers used to describe the Al slab should be much larger (> 40). These deviations are usually attributed to quantum effects which decrease very slowly with the number of atomic layers [49]. The calculations with a 40-layers slab being too computationally expensive, we checked that the three methods give interlayer distance deviations that are in the same range of values for the 19-layers slab and can be compared. For the other systems, the interlayer distances converge to the bulk value in the middle of the slab with an incertainty of less than $\pm1\%$.

It is interesting to notice that the surface relaxations, measured by the Δd_{12} and Δd_{23} deviations of the interlayer distances, can be very different from one method to the other for a given metal. These surface relaxations are reported in table 8.

Some experimental studies in the literature have shown that for most of the fcc metals, the surface relaxation is inward, i.e. the distance between the two topmost atomic layers decreases when compared to this distance in the bulk. But, some surfaces show an outward relaxation such as Al(111) and Au(111) or Cu(111) [50–52]. Since experimental values are difficult to obtain with a reasonable uncertainty, the prediction of this opposite behavior could be considered to evaluate the performance of the dispersion corrected approaches.

For Al(111), the calculated Δd_{12} is positive for the three methods, i.e. PBE, DFT-D2 and optB86b but it is much increased by the use of the vdW functionals, especially DFT-D2. This outward relaxation agrees with the experimental observations and within acceptable errors for PBE and optB86b. For Cu(111), both PBE and optB86b give a negative (inward) relaxation. Only the DFT-D2 reproduce the outward behavior with $\Delta d_{12} = +0.74\%$.

For Au(111), all methods reproduce the outward relaxation observed experimentally [51] but its magnitude is much bigger for the DFT-D2 method. The Ni(111) surface shows experimentally an inward relaxation, which is reproduced by the three methods. However, the optB86b value (–1.31%) agrees better with the –1.2% $\pm$ 1.2% estimated by Lahtinen $et\ al$ [56]. For the Co(0001) surface, all methods reproduce the inward relaxation. Finally
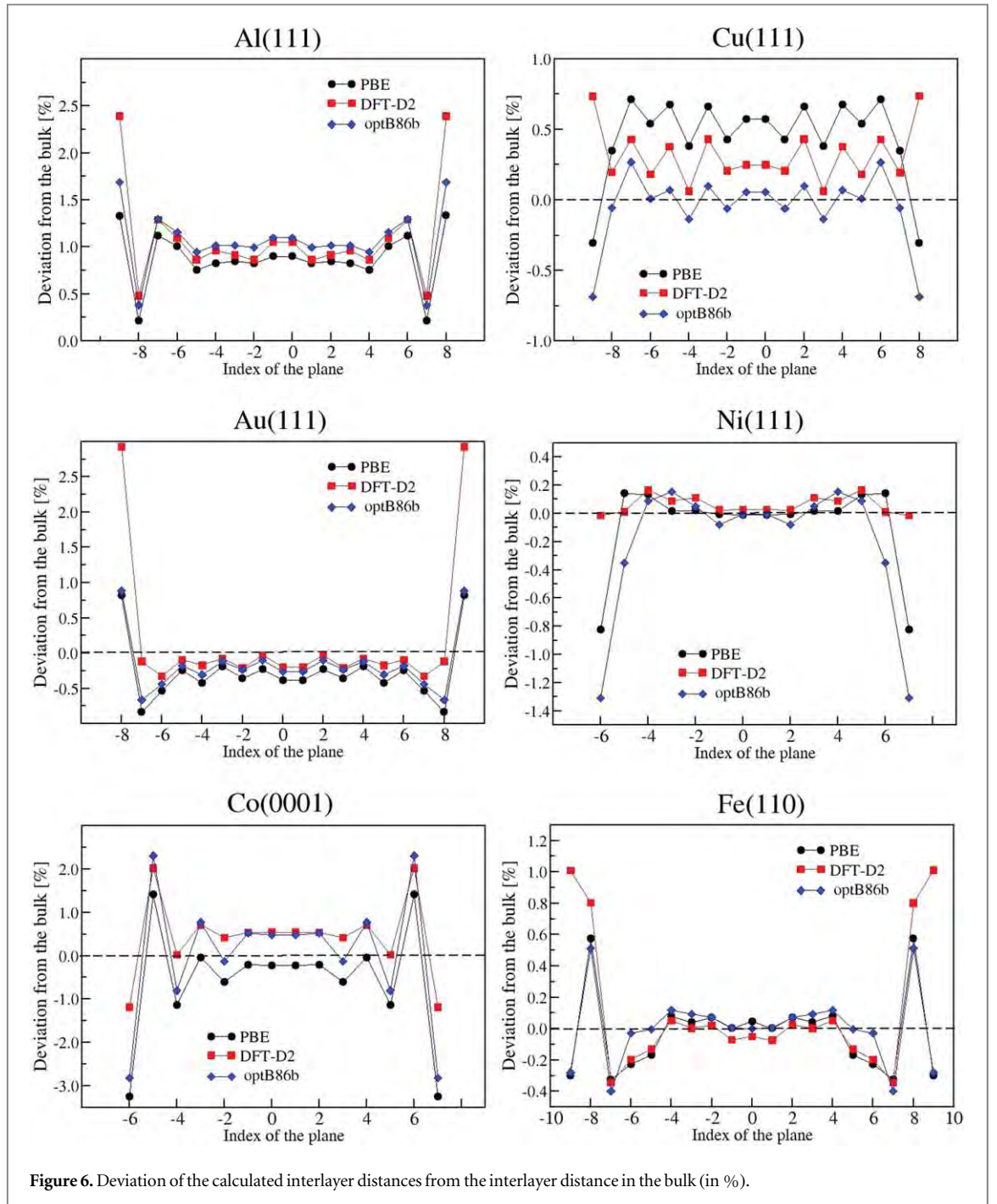
Figure 6. Deviation of the calculated interlayer distances from the interlayer distance in the bulk (in %).

for the Fe(110) surface, the DFT-D2 method gives an outward relaxation (+1.01%), while PBE and optB86b simulate an inward relaxation of −0.29% and −0.18% respectively.

For all metals, the agreement with experiment is difficult to evaluate because of the dispersion of the experimental values. Globally, we note that for the Δd_{12} variation, the PBE and optB86b functional show the same trends whereas DFT-D2 has a different behavior for Cu(111) and Fe(110). These trends and the comparisons with experimental values are shown in figure 7, where the Δd_{12} are depicted. From this figure, it is clear that the DFT-D2 method tends to increase the surface deviation Δd_{12} compared to the PBE and optB86b ones and this effect changes the relaxation from inward to outward in some cases (Cu(111) and Fe(110)).

For magnetic surfaces, the magnetic moment of atoms belonging to the different layers shows a similar variation for the three methods (see figure 8). Similarly to what was observed in the bulk, the decrease of the lattice parameter when the dispersive forces are included induces a decrease of the atomic magnetic moment in the middle of the slabs. At the surface, due to the lack of neighbouring atoms, the magnetic moment of the surface atoms is exalted. This exaltation is obtained with the three functionals and the differences between the obtained values are simply due to the change in bulk atomic moments.
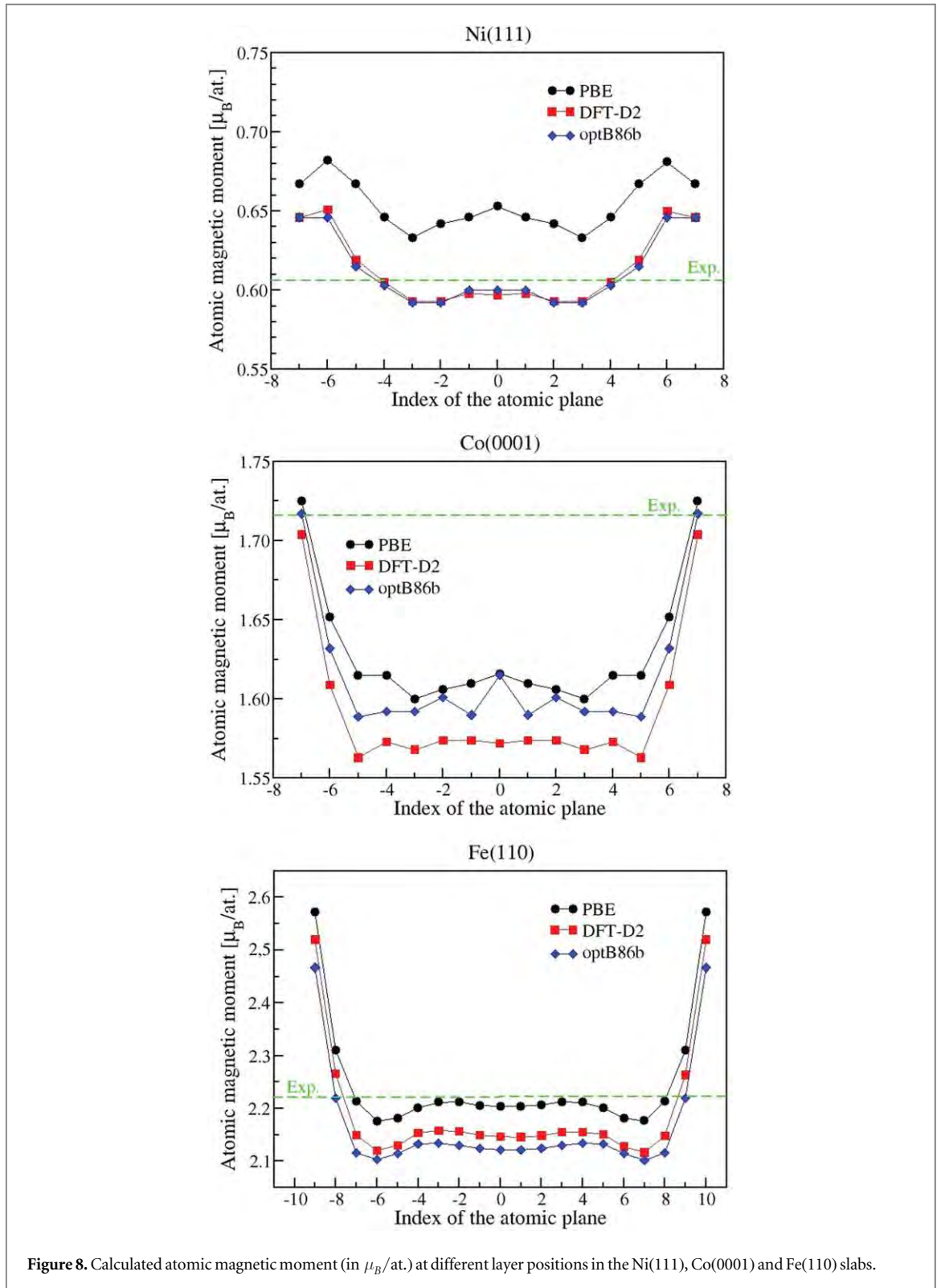
Table 8. Calculated and experimental deviation of the interlayer distances Δd_{12}, Δd_{23}, and Δd_{34}, from the corresponding bulk values (in %).

Element	PBE	DFT-D2	optB86b	Exp.
Al(111)				
Δd_{12}	+1.34	+2.39	+1.69	+1.8 ± 0.3/ +1.7 ± 0.3 [50, 53]
Δd_{23}	+0.22	+0.48	+0.38	+0.1 ± 0.7/ 0.5 ± 0.7 [50, 53]
Δd_{34}	+1.12	+1.29	+1.29	
Cu(111)				
Δd_{12}	−0.30	+0.74	−0.68	+0.5 − 1 ± 1 − 2.5% [52]
Δd_{23}	+0.35	+0.19	−0.06	
Δd_{34}	−0.71	+0.43	+0.27	
Au(111)				
Δd_{12}	+0.82	+2.93	+0.89	+1.5/ +3.3 ± 0.4 [51, 54]
Δd_{23}	−0.84	−0.12	−0.66	−0.8 ± 0.4 [54]
Δd_{34}	−0.53	−0.33	−0.44	
Ni(111)				
Δd_{12}	−0.82	−0.11	−1.31	−1.2 ± 1.2 [55]
Δd_{23}	+0.14	−0.05	−0.35	
Δd_{34}	+0.13	−0.09	+0.09	
Co(0001)				
Δd_{12}	−3.24	−1.18	−2.81	−2.1 [56]
Δd_{23}	+1.41	+2.02	+2.30	+1.3 [56]
Δd_{34}	−1.13	+0.03	−0.80	
Fe(110)				
Δd_{12}	−0.29	+1.01	−0.18	+0.5 ± 2 [57], +1 ± 2 [58]
Δd_{23}	+0.57	+0.80	+0.54	+0.5 ± 2 [58]
Δd_{34}	−0.32	−0.34	−0.36	
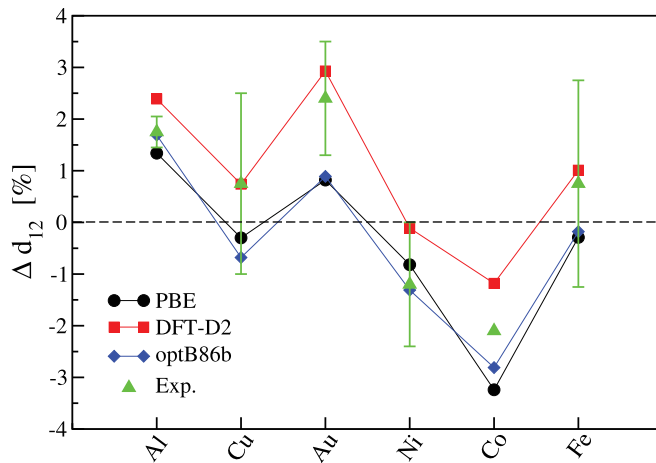
Figure 7. Surface relaxations Δ_{12} with respect to the bulk interlayer distances (in %) and comparison with the experimental values.

To summarize, similarly to the bulk properties, the variation trend of surface properties using PBE, DFT-D2 and optB86b methods strongly depends on the system. For the surface energy, it is clear that the use of the dispersion forces increases the value of the surface energy when compared to the PBE results, for all metals. The method dependence of the work function is different with a systematic increase of the value using the optB86b functional. But the use of the DFT-D2 method does not affect systematically the PBE value of the work function.

Figure 8. Calculated atomic magnetic moment (in μ_B/at.) at different layer positions in the Ni(111), Co(0001) and Fe(110) slabs.

Concerning the surface relaxation, the DFT-D2 method clearly increases the interlayer distance between the topmost layers. However the comparison with experiments is not conclusive. For what concerns the surface magnetic moments, the trend follows that found for the bulk magnetic moment, i.e. it is closely related to the lattice parameter.

4. Conclusion

In this paper, we have evaluated the performance of two vdW-corrected DFT functionals (DFT-D2 and vdW–DF/optB86b) on six metals, i.e. Al, Cu, Au, Ni, Co and Fe by comparing with PBE results and experiments. A systematic decrease of the lattice parameter compared to the PBE value was observed which is directly related to the inclusion of the attractive dispersion forces in the metal. For the same reasons, the cohesive energy is systematically increased in absolute value and the magnetic moment is decreased when vdW corrected functionals are used, with respect to PBE. Based on the investigated metals (including transition 3d/5d metals), one could generalize this trend: the use of vdW corrected DFT induces a decrease of the lattice parameter, a decrease of the magnetic moment and an increase of the cohesive energy in absolute values with respect to standard GGA–DFT calculations. However, for the bulk moduli which is linked to the elastic properties of the materials, no general trend could be found.

Surface energies, work functions and surface relaxations of Al(111), Cu(111), Au(111) and magnetic Ni(111), Co(0001) and Fe(111) surfaces were computed with and without the vdW corrections. A variation trend was underlined for the surface energy: $\gamma_{PBE} < \gamma_{optB86b} < \gamma_{DFT-D2}$, which can be attributed to the changes in the bulk properties. Concerning the work function, the ordering is different and the trend is: $\Phi_{PBE} \leqslant \Phi_{DFT-D2} < \Phi_{optB86b}$. For surface relaxations, the DFT-D2 correction tends to increase the distance between the two topmost layers compared to the very similar behavior found with PBE and the optB86b functionals.

A proper description of molecule/surface systems implies to take into account London dispersion forces which is not done in standard GGA–DFT calculations. The state-of-the-art vdW corrected functionals are now routinely used to overcome this failure of DFT. Care should be taken regarding the effects induced by these forces on the metal properties. In this work, we have observed that the use of vdW corrected functionals strongly affects the bulk and surface properties of the investigated metals. In order to avoid this effect, for semi-empirical corrections based on pairwise additive interactions, one could introduce the corrections between the atoms of the molecule and of the surface only [59]. This strategy can not be used for non-local vdW corrected functionals. In this latter case, the general trends pointed out in the present study could be used to predict the change of the metal properties with respect to standard DFT.

References

[1] Eisenschitz R and London F 1930 *Z. Phys.* **60** 491
[2] Rehr J J, Zaremba E and Kohn W 1975 *Phys. Rev.* B **12** 2062
[3] Mahanty J and Taylor R 1978 *Phys. Rev.* B **17** 554
[4] Upadhyaya J C 1981 *Solid State Commun.* **38** 415
[5] Maggs A C and Ashcroft N W 1987 *Phys. Rev. Lett* **59** 113
[6] Jurečka P, Šponer J, Černý J and Hobza P 2006 *Phys. Chem. Chem. Phys* **8** 1985
[7] Distasio R A Jr, Gobre V V and Tkatchenko A 2014 *J. Phys.: Condens. Matter* **26** 213202
[8] Reilly A M and Tkatchenko A 2012 *J. Chem. Phys* **139** 024705
[9] Klimeš J and Michaelides A 2012 *J. Chem. Phys* **137** 120901
[10] Tafreshi S, Roldan A and de Leeuw N H 2015 *Surf. Sci.* **637-638** 140–8
[11] Berland K, Cooper V R, Lee K, Schröder E, Thonhauser T, Hyldgaard P and Lundqvist B I 2015 *Rep. Prog. Phys* **78** 66501
[12] Becke A D 2014 *J. Chem. Phys* **140** 18A301
[13] Burns L A, Vázquez-Mayagoitia A, Sumpter B G and Sherrill C D 2011 *J. Chem. Phys.* **134** 084107
[14] Tao J, Perdew J P and Ruzsinszky A 2013 *Int. J. Mod. Phys.* B **27** 1330011
[15] Liu W, Tkatchenko A and Scheffler M 2014 *Acc. Chem. Res.* **47** 3369
[16] Liu W, Friedrich M, Willenbockel M, Bronner C, Schulze M, Soubatch S, Tautz F S, Tegeder P and Tkatchenko A 2015 *Phys. Rev. Lett.* **115** 036104
[17] Klimeš J, Bowler D R and Michaelides A 2010 *J. Phys.: Condens. Matter* **22** 022201
[18] Klimeš J, Bowler D R and Michaelides A 2011 *Phys. Rev.* B **83** 195131
[19] Carrasco J, Liu W, Michaelides A and Tkatchenko A 2014 *J. Chem. Phys.* **140** 084704
[20] Schimka L, Gaudoin R, Klimeš J, Marsman M and Kresse G 2013 *Phys. Rev.* B **87** 214102
[21] Ding Z, Liu W, Li S, Zhang D, Zhao Y, Lavernia E J and Zhu Y 2016 *Acta Mater.* **107** 127
[22] Bucko T, Lebègue S, Hafner J and Angyan J G 2013 *Phys. Rev.* B **870** 064110
[23] Tkatchenko A and Scheffler M 2009 *Phys. Rev. Lett.* **102** 073005
[24] Gattinoni C and Michaelides A 2015 *Faraday Discuss.* **180** 439–58
[25] Tereshchuk P, Chaves A S and Da Silva J L F 2014 *J. Phys. Chem.* C **118** 15251–9

[26] Tarrat N, Benoit M, Giraud M, Ponchet A and Casanove M J 2015 *Nanoscale* **7** 14515
[27] Baltrusaitis J, Valter M and Hellman A 2016 *J. Phys. Chem.* C **120** 1749
[28] Gece G 2011 *Corros. Sci.* **53** 3873
[29] Langlois C, Benzo P, Arenal R, Benoit M, Nicolai J, Combe N, Ponchet A and Casanove M J 2015 *Nano Lett.* **15** 5075
[30] Ait Atmane K, Michel C, Piquemal J-Y, Sautet P, Beaunier P, Giraud M, Sicard M, Nowak S, Losnoe R and Viauf G 2014 *Nanoscale* **6** 2682
[31] Kresse G and Hafner J 1993 *Phys. Rev.* B **47** 558
[32] Kresse G and Furthmuller J 1996 *Phys. Rev.* B **54** 11169
[33] Kresse G and Furthmuller J 1996 *Comput. Mater. Sci.* **6** 15
[34] Kresse G and Joubert D 1999 *Phys. Rev.* B **59** 1758
[35] Blochl P E 1994 *Phys. Rev.* B **50** 17953
[36] Perdew J P, Burke K and Ernzerhof M 1996 *Phys. Rev. Lett.* **77** 3865
[37] Grimme S 2006 *J. Comput. Chem.* **27** 1787
[38] Dion M, Rydberg H, Schröder E, Langreth D C and Lundqvist B I 2004 *Phys. Rev. Lett.* **92** 246401
[39] Methfessel M and Paxton A T 1989 *Phys. Rev.* B **40** 3616
[40] Monkhorst Hendrik J and Pack James D 1976 *Phys. Rev.* B **13** 5188
[41] Murnaghan F D 1944 *Physics* **30** 244
[42] Silva Da 2006 *Surf. Sci.* **600** 703
[43] Kittel C 2005 *Introduction to Solid State Physics* 8th edn (New York: Wiley)
[44] Galperin F M 1973 *Phys. Status Solidi* b **57** 715
[45] Wakiyama T 1971 *J. Phys. Colloques* **32** 340
[46] Skriver H L and Rosengaard N M 1992 *Phys. Rev.* B **46** 7175 and reference therein
[47] Ferri N, DiStasio J, Robert A, Ambrosetti A, Car R and Tkatchenko A 2015 *Phys. Rev. Lett* **114** 176802
[48] Ibach H 1997 *Surf. Sci. Rep.* **29** 193–263
[49] Da Silva Juarez L F 2005 *Phys. Rev.* B **71** 195416
[50] Noonan J R and Davis H L 1990 *J. Vac. Sci. Technol.* A **8** 2671
[51] Nichols R J, Nouar T, Lucas C A, Haiss W and Hofer W A 2002 *Surf. Sci.* **513** 263
[52] Bartos I, Jaros P, Barbieri A, Hove M A V, Chung W F, Cai Q and Altman M S 1995 *Surf. Rev. Lett.* **2** 477
[53] Stampfl C, Scheffler M, Over H, Burchhardt J, Nielsen M, Adams D L and Moritz W 1994 *Phys. Rev.* B **49** 4959
[54] Sandy A R, Mochrie S G J, Zehner D M, Huang K G and Gibbs D 1991 *Phys. Rev.* B **43** 4667
[55] Demuth J E, Marcus P M and Jepsen D W 1975 *Phys. Rev.* B **11** 1460
[56] Lahtinen J, Vaari J, Vaara T, Kauraala K, Kaukasoina P and Lindroos M 1999 *Surf. Sci.* **425** 90
[57] Shih H D, Jonat F, Bardit U and Marcus P M 1980 *J. Phys. C: Solid State Phys.* **13** 3801
[58] Xu C and OConnor D J 1991 *Nucl. Instrum. Methods Phys. Res.* **B53** 315
[59] Chiter F, Lacaze-Dufaure C, Tang H and Pébère N 2015 *Phys. Chem. Chem. Phys* **17** 22243